

The Numerical Simulation of Equivalent Static Pressures Distribution for the Aircraft Tire Burst Jets Based on MATLAB

Runlian Jiang^{1,2}, Yaohua Wang¹, Chengfei Fan¹ and Mianjun Duan¹

¹College of Field Engineering, PLA Univ. of Sci. &Tech
Hai Fu Xiang Street 1, Nanjing, Jiangsu, 210007, China

²Zhenjiang Watercraft College of PLA, Zhenjiang, Jiangsu, 212003 China

bestlian@163.com, 2282182762@qq.com, 598789085@qq.com, 377583360@qq.com

Abstract

The dynamic pressures at a distance of 500mm away from the spout for the aircraft tire burst jets were measured in the aircraft main landing gear. The dynamic pressures were treated for equivalent static pressures while the distributions of the equivalent static pressures were simulated by linear and cubic spline interpolation functions based on MATLAB software. The results showed that the equivalent static pressure close to the middle region of the sector is relatively large at the same distance from the spout. The distributions by linear interpolation are more uniform than cubic spline interpolation, but the results from the cubic spline interpolation are more rounded than the other. The equivalent static pressure less 500mm away from the spout was obtained by the interpolations. Moreover, the equivalent static pressures are usually higher by cubic spline interpolation than linear interpolation.

Keywords: Aircraft tire burst, Jet, Equivalent static pressure, numerical simulation

1. Introduction

The aircraft tire is a very important part with high requirements in safety and reliability. The safety of aircraft taking off and landing must rely on a variety of unique features of the aircraft tire. The smaller volume of the tire, the greater efficient space the aircraft has. The lighter weight of the tire, the greater effective load the aircraft carries. This requires that the tire has very high load capacity that guaranteed by a high inflation pressure. The tire pressure inside the aircraft tire is 1.73MPa at the normal working hours comparing to the “rubber bomb”.

The bead filler rubber of the aircraft tire is relatively thick. The tire has many characteristics, for example, high load, high inflation pressure, large heat generation, high speed, short sliding distances and so on. These characteristics cause bursting due to internal or external object stab fever. Accidental bursting would threaten the airframe, the fuel tank and engine safety. Bai Jie analyzed formation mechanism and speed of aircraft tire burst debris and acquired velocity calculation model of the tire fragments [1]. While the aircraft parts, pipes in the aircraft main landing gear compartment will be impacted by a powerful shockwave dynamic load. Therefore, it is very necessary to research the dynamic strength of

the equipments and pipes which are in the aircraft main landing gear compartment. To ensure that the key parts in the main landing gear compartment are not damaged by the impacts of the tire burst jets requires that key parts to be designed in accordance with the most severe airworthiness status and analyzed dynamic strength [2, 3]. Due to test conditions limitation, the shock wave pressure data of the tire burst jets was obtained at the measuring locations which are more than 500mm away from the spout, but the most parts are less 500mm away from the spout. According to the equivalent static pressure distribution that was over 500mm away from the spout, the equivalent static pressure data less 500mm away from the spout was obtained by the interpolations in this paper. These outcomes provide bases for design and manufacture of the key parts in the main landing gear compartment for the model aircraft.

2. Pressure Measurement of the Aircraft Tire Burst Jets

2.1 Setting aircraft tire burst test

The tire burst modes are clearly defined in JAA standards. In this section, the tire is not rotating, gear is retracted, the energy considered is the one coming from the blast effect. In this approach, the debris size is random.

Assuming that jet field space being relatively small, the principles which do not interfere with the original state jet field and reduce the mutual interference among the sensors must be followed. The reflected pressure sensors are selected in the tests. Tire bursts impacting airflows are referred as jets. The jet field should be a conical shape [4]. The jets spread to a sector in the horizontal direction and the spout center is the apex of the sector in the test. Central angle of the sector is 72° . The fifteen pressure sensors are positioned consistent with the locations specified on Figure 1 and 2. Moreover, the external pressure sensor is 300psi range while the sensor is 500psi range in the tire for measuring pressure changes. The total pressure of sensors is 16. Due to the constraints of test conditions, the test sensors are all positioned the locations more than 500mm away from the spout.

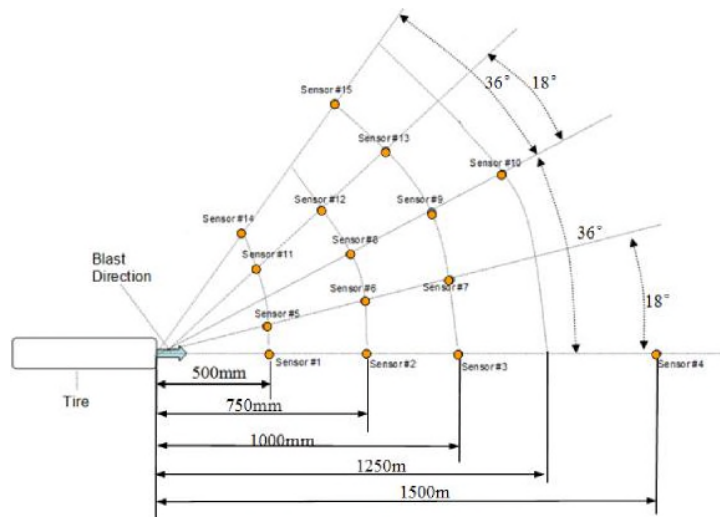


Figure 1. Locations of pressure sensors (side view)

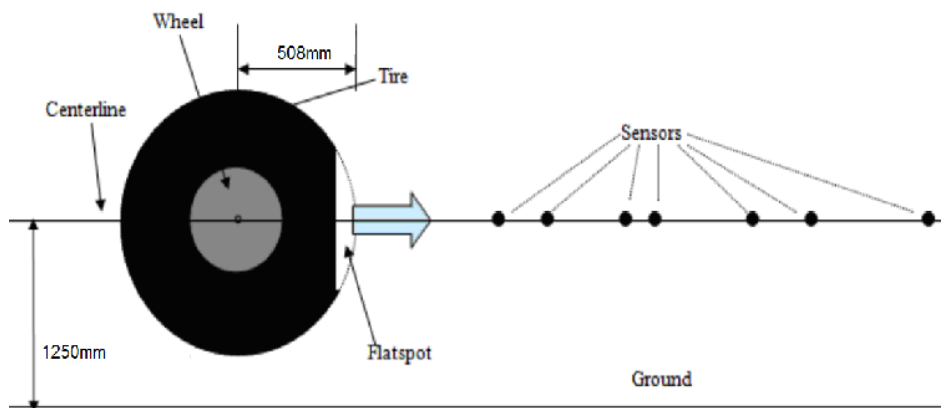


Figure 2. Locations of pressure sensors (top view)

The energy will be determined by measurement. Through a static burst test, the jet pattern will be visualized, and the energy of the jet with the data from the pressure sensors will be calculated as well. A hot wire method was developed during this test to cut the tires and initiate the tire burst. The pressure sensors were utilized to capture the burst jet pressure.

The stored energy can be determined by calculation and the method was proposed by Grumman to NASA in 1965. The stored energy in a Pressure Vessel equation are as follows:

(1)

Where U : energy [J]

F1: inflated pressure [Mfa]

F2: final pressure [Mfa]

V : volume [cm^3]

k : gas constant [1.41 for N_2 or air]

Input: $F_1 = 1.825Mfa$, $F_2 = 0.101Mfa$, $V = 138000 cm^3$, Result: $U = 3.5 \times 10^5 J$.

If the tire burst, the powerful energy is released instantaneously, the key parts in the main landing gear compartment will be impacted and damaged by the jets.

2.2 The tire burst jets pressures distribution in tests

Figure 3 shows the pressure curve of each sensor in test 3. The peak pressure closes to the explosion is difficult to measure and grasp accuracy in the current test levels [5]. The tire pressure is 250psi at the beginning of the burst. The pressure value of sensor in the tire sharp decline as the blast wave spreads. The peak pressures of the 1st and the 5th sensors are larger in the shock wave spreading at the first 2ms. The peak pressure of the 8th sensor is larger in 2-4ms. Then the peak pressure of the 8th sensor is larger in 2-4ms. The peak pressures of 11th and 14th sensor reach the maximum in 4-6ms. It shows that shock waves of the tire burst spread along the fan-shaped. The shock waves interacting with the reflected shock waves make the loads of the peak pressures and momentums acting on the structure increased when the incident and reflected waves coupled to each other, it causes a small

fluctuations to the peak pressure [6]. The farther from the tire, the lower the peak pressure of the sensor is.

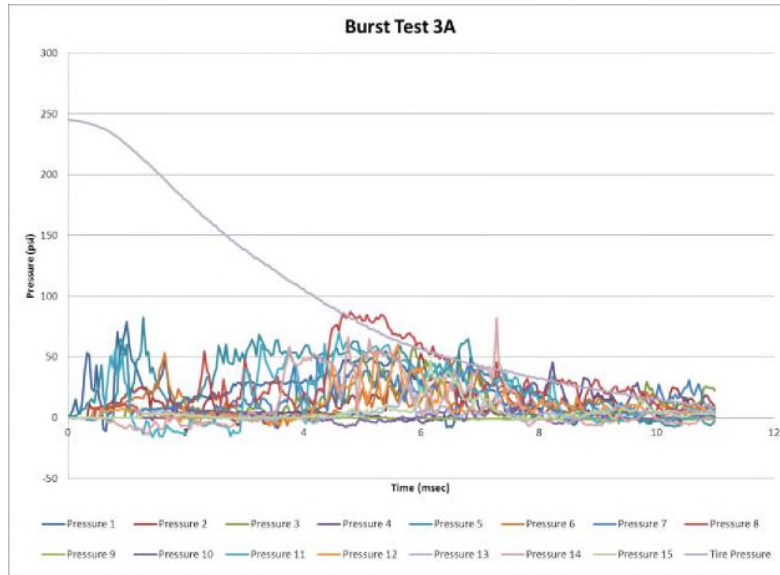


Figure 3. Each sensor pressure curve in test 3

In order to monitor the pressure release within the tire in tests, the range of 500psi piezoelectric pressure sensor was defined near the spout for measuring pressure changes in the tire. The pressure curve of the 16th sensor in the tire is shown on figure 3. It is 10.5ms for the pressure of the sensor 16 releasing to 12.5 psi on figure 3. The pressure released rapidly at first because of the most different pressure of inside and outside tires. The tire pressure has released 80% when the tire burst time is 6ms.

0

2.3 Equivalent static pressures distributions in tests

The equivalent static pressure is calculated based on the dynamic pressure curve. The equivalent static pressure is the area under the dynamic pressure curve divided by the duration of the pressure pulse which corresponds to the average pressure during the burst at the location of the sensor.

The integral of the pressure is: (2)

$$P(t)dt$$

□

0

It's represented by the area under the curve on Figure 4(orange area).

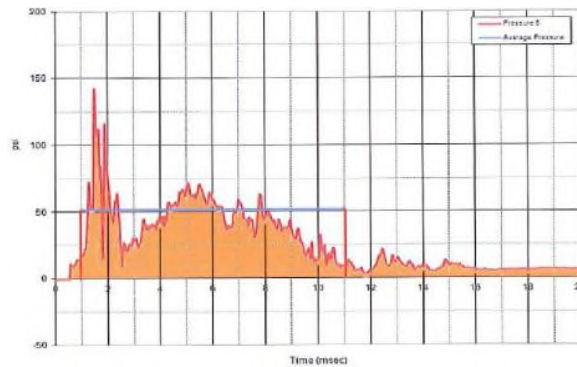


Figure 4. Equivalent static pressure

∅

□

∅

The static designs of the structures in the aircraft main landing gear compartment are originally based on the equivalent static pressures of the tire burst jets. Simultaneously, the equivalent static pressures are loaded into the key parts in the landing gear compartment for subsequent dynamic strength check. Equivalent static pressure is equivalent to the average pressure in bursting process for a period of time. Considering that tire burst has a duration of $\Delta t=10\text{ms}$, the time for the pressure reaches 5% of its initial value. The equivalent static pressure equation as in

(3)

The equivalent static pressure is represented by the blue line on Figure 4. The test data was dealt with by using (2) based on MATLAB software. The equivalent static pressures of the fifteen sensors are given in Table 1. Considering the aircraft safety, the maximum pressure of the six tests is regarded as the calculation data of equivalent static. Figure 4 shows the comparison between maximum equivalent static pressures and the distance of the sensor positions from the spout. Maximum static pressure decreases with increasing distance between measuring point and the spout on Figure 5.

Table 1. Equivalent static pressure (PSI)

sensor	Test1	Test2	Test3	Test4	Test5	Test6	Max
1	54.01	22.39	17.66	27.50	35.70	51.53	54.01
2	14.93	17.08	21.47	29.27	28.02	21.36	29.27
3	17.27	15.47	19.88	18.57	15.41	11.91	19.88

4	9.47	7.25	9.90	5.98	5.74	3.54	9.90
5	51.64	45.90	31.47	27.65	39.93	54.81	54.81
6	6.36	17.46	18.70	25.24	28.63	25.81	28.63
7	16.69	14.77	21.22	17.14	19.25	12.79	21.22
8	28.60	42.66	33.88	50.78	35.85	33.48	50.78
9	6.59	19.88	10.00	14.13	11.79	9.57	19.88
10	5.36	10.04	4.22	7.09	5.24	4.24	10.04
11	18.33	37.23	18.22	20.93	28.86	28.05	37.23
12	6.50	15.53	14.29	14.39	12.94	9.01	15.53
13	6.02	9.68	6.39	7.15	7.24	5.38	9.68
14	6.88	5.38	10.52	16.13	12.95	15.34	16.13
15	4.65	6.12	6.99	5.94	4.45	5.81	6.99

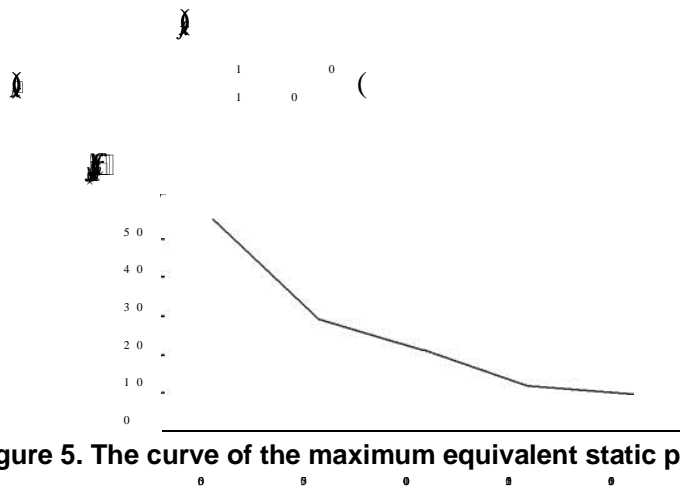


Figure 5. The curve of the maximum equivalent static pressures

3. The Numerical Simulation of Equivalent Static Pressures Distribution

3.1 Interpolation method introduction

The interpolation is an important method for function [approximation](#) as well as estimating the function in the other point values through the function in the finite point value. The equivalent static pressure is estimated by linear and cubic spline interpolation methods in the tire burst tests.

1. Linear interpolation function

If coordinates (x_0, y_0) and (x_1, y_1) were known, we could have obtained the values on the line in the interval $[x_0, x_1]$ at x position. The function of the linear interpolation function as in

$$y = \frac{y_1 - y_0}{x_1 - x_0}(x - x_0) + y_0 \quad (4)$$

2. Cubic spline interpolation function
Cubic spline function denotes by $s(x)$, which is defined in the interval $[a, b]$ [7]. The function met

$$s(x) = \sum_{i=0}^{n-1} p_i(x)$$

times polynomial

in each sub

■

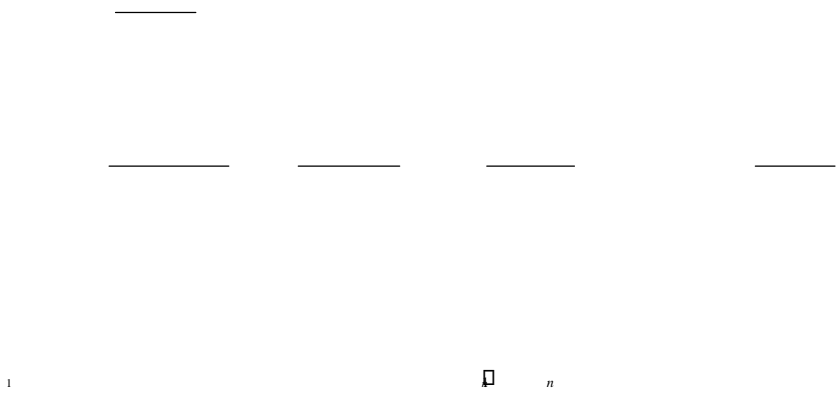
□

Where

$$\begin{aligned}
 & \left[\begin{array}{c} \dot{x}_1 \\ \dot{x}_2 \\ \vdots \\ \dot{x}_n \end{array} \right] = \left[\begin{array}{c} a_{11} \\ a_{21} \\ \vdots \\ a_{n1} \end{array} \right] x_1 + \left[\begin{array}{c} a_{12} \\ a_{22} \\ \vdots \\ a_{n2} \end{array} \right] x_2 + \dots + \left[\begin{array}{c} a_{1n} \\ a_{2n} \\ \vdots \\ a_{nn} \end{array} \right] x_n + \left[\begin{array}{c} b_1 \\ b_2 \\ \vdots \\ b_n \end{array} \right] u \\
 & y = \left[\begin{array}{c} c_1 \\ c_2 \\ \vdots \\ c_n \end{array} \right] \left[\begin{array}{c} x_1 \\ x_2 \\ \vdots \\ x_n \end{array} \right] + d u
 \end{aligned}$$

$$\left[\begin{array}{c} \dot{x}_1 \\ \dot{x}_2 \\ \vdots \\ \dot{x}_n \end{array} \right] = \left[\begin{array}{c} a_{11} \\ a_{21} \\ \vdots \\ a_{n1} \end{array} \right] x_1 + \left[\begin{array}{c} a_{12} \\ a_{22} \\ \vdots \\ a_{n2} \end{array} \right] x_2 + \dots + \left[\begin{array}{c} a_{1n} \\ a_{2n} \\ \vdots \\ a_{nn} \end{array} \right] x_n + \left[\begin{array}{c} b_1 \\ b_2 \\ \vdots \\ b_n \end{array} \right] u$$

1 2



The cubic spline interpolation function in the interval

as

(8) **3.2 The**

equivalent static data interpolation based on MATLAB

Figure 1 indicates that most of the test pressure sensors distribute fan-shaped. But the key parts are less 500mm away from the spout. The 2nd and 4th sensors can be ignored because the two sensors are located far away from the spout.

Testing data of the two sensors is lacking. One is located in the direction of 35 ° at radius of 500mm while the other one is located in the direction of 70 ° at radius of 750mm. The two positions in the sector area are influenced by jet flow. The testing data of the two sensors directly influences the final interpolation results. And the first one is more important than the other one.

In order to solve the lack of test data of the sensors, we have made some assumptions in the flow field to the pressure value being proportional to the radius linearly decrease along the ray direction. So the missing pressure data of two locations is obtained by interpolation in adjacent sensors data along the ray direction. Thus these two pressure values are obtained by interpolating as follows:

Direction at 35 ° radius 500mm: ,

Direction at 70 ° radius 750mm: .

The six test data shows that the tire burst process has great randomness, causing the jet field pressure differs at the same position in different tests. So the interpolation is mainly carried out in the test data of the same test. Interpolation is a two-dimensional function in the polar coordinate. The function value depends on two parameters in MATLAB. More specially, the two parameters are the distance from the measuring point to spout r and the angle O [8]. The codes to achieve linear interpolation are as follow:

```
maxload_linear=[];
for j=1:1:6
figure
```

```
[r,theta]=meshgrid(25.4*20:25.4*10:25.4*40,0:17.5*pi/180:70*pi/180);
r0=zeros(5,1);
r=[r0 r];
th1=theta(:,1);
theta=[th1 theta];
x=r.*cos(theta);
y=r.*sin(theta);
for i=1:1:5
z(i,1)=average(16,j);
end
```

```
z(1,2)=average(1,j); z(1,3)=average(2,j);  
z(1,4)=average(3,j); z(2,2)=average(5,j);  
z(2,3)=average(6,j); z(2,4)=average(7,j);  
z(3,2)=(average(16,j)+2*average(8,j))/3;  
z(3,3)=average(8,j);  
z(3,4)=average(9,j);  
z(4,2)=average(11,j);  
z(4,3)=average(12,j);  
z(4,4)=average(13,j);  
z(5,2)=average(14,j);  
z(5,3)=(average(14,j)+average(15,j))/2;  
z(5,4)=average(15,j);  
  
[ri,thetai]=meshgrid(0:25.4*1:25.4*40,0:17.5*pi/(5*180):70*pi/180);  
zi = interp2(r,theta,z,ri,thetai);  
xi=ri.*cos(thetai);  
yi=ri.*sin(thetai);  
surf(xi,yi,zi)  
r1=[320 100 380 140 300 130 400];  
theta1=[0:17.5*pi/(5*180):70*pi/180];  
[r2,theta2]=meshgrid(r1,theta1);  
z2 = interp2(ri,thetai,zi,r2,theta2);  
maxload1=max(z2,[],1);  
maxload_linear=[maxload_linear; maxload1];  
end
```

3.3 Distributions of the equivalent static pressures in tests

There is a great randomness of the tire burst process from the test results. The pre-worn state of the tire caused the changes of spout sizes and expansion speeds in different tests and thus resulted in different pressures at the same location in different tests. But the flow field of the same test is determined. Therefore, the interpolation is studied among the data from the same test. Besides, the equivalent static pressure for the unknown region is estimated. The maximum is taken as the final estimated value by consolidating the six tests interpolation estimate results. The interpolation algorithms are composed of linear and spline interpolation algorithm and the best estimation is selected according to the analysis of the space distribution of the two interpolation results.

The polar coordinate transforms into the Descartes coordinate system for graphical display after interpolated. The simulation results of the equivalent static pressures by linear and cubic spline interpolation are shown on figure 6 and 7 for 6 tests.

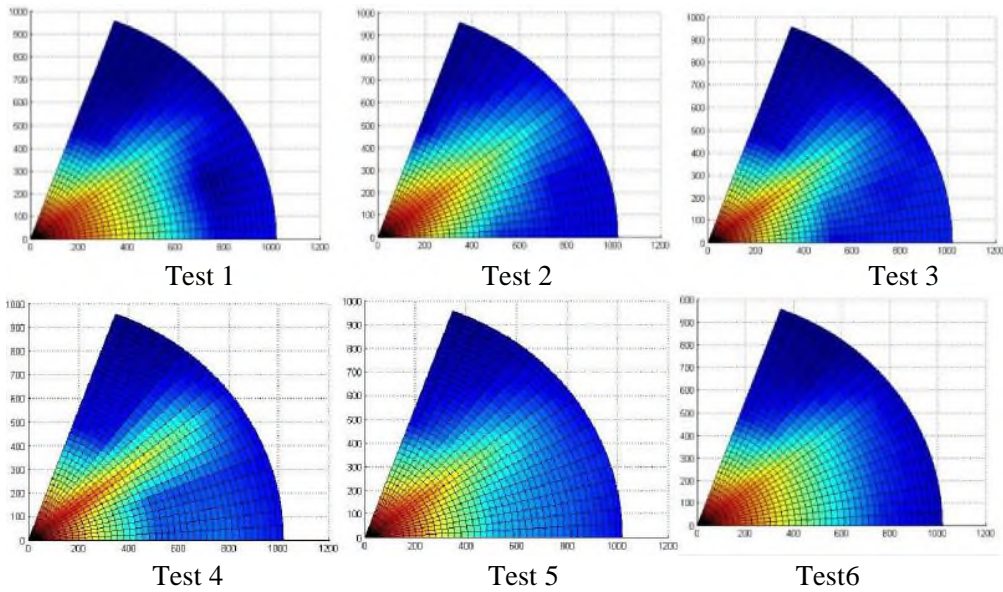


Figure 6. Cloud charts of equivalent static pressures distribution by linear

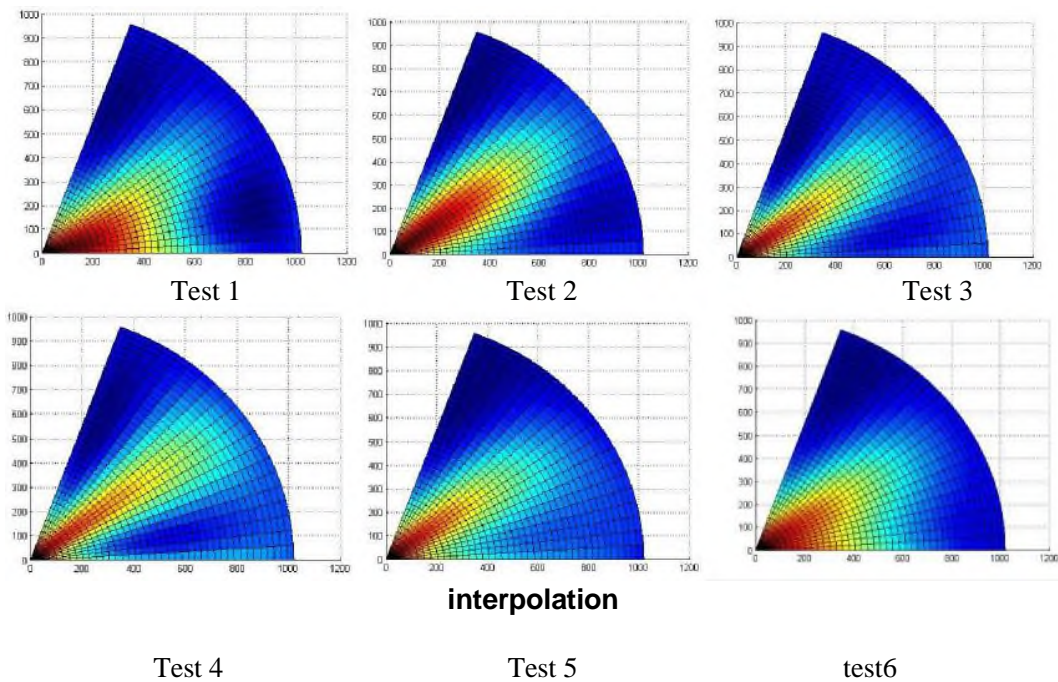


Figure 7. Cloud charts of equivalent static pressures distribution by spline interpolation

The equivalent static pressures are different at the same distance from the spout with different angle from the view of spatial distributions on Figure 5 and Figure 6. The equivalent static pressure is greater near the middle region of the sector. Meanwhile, the pressures distribution is uniformed by the linear interpolation. The pressures distribution is smooth, but the higher pressure area is relatively concentrated by spline interpolation [9, 10].

3.4 Interpolation results of equivalent static pressure at the key parts

The key parts in the main landing gear compartment are less 500mm from the spout. The pressures can not be measured in the tire burst tests at the key parts while the key parts in the design should be based on equivalent static pressure. Regarding the test data, the flow field pressures are different at different directions at a radius in the same test. To obtain the maximum equivalent static pressure, the pressures should be investigated in different angles on the interpolation results in the same distance. Considering the aircraft safety, take maximum interpolation results of the six tests as the following key parts design basis. Equivalent static pressure by linear and spline interpolation are given in Table 2 and 3. Figure 8 shows the maximum equivalent static pressures in six tests at critical parts by the linear and spline interpolation versus the distance of the critical parts from the spout.

Table 2. Equivalent static pressure at the key parts by linear interpolation (PSI)

distances	Test 1	Test 2	Test 3	Test 4	Test 5	Test 6	Max
100mm	99.32	99.69	94.00	102.41	99.16	106.12	106.12
130mm	96.11	97.11	91.28	100.07	96.29	102.83	102.83
140mm	95.04	96.25	90.37	99.29	95.33	101.74	101.74
300mm	77.95	82.46	75.84	86.81	80.03	84.18	86.81
320mm	75.81	80.74	74.02	85.25	78.12	81.98	85.25
380mm	69.40	75.57	68.57	80.57	72.38	75.40	80.57
400mm	67.27	73.84	66.75	79.01	70.47	73.20	79.01

Table 3. Equivalent static pressure at the key parts by spline interpolation (PSI)

distances	Test 1	Test 2	Test 3	Test 4	Test 5	Test 6	Max
100mm	117.24	101.41	94.49	98.94	99.21	108.34	117.24
130mm	116.67	98.88	91.83	96.07	96.34	105.44	116.67
140mm	116.23	97.99	90.94	95.17	95.39	104.45	116.23
300mm	95.80	83.12	76.25	83.11	80.08	87.25	95.80
320mm	91.94	81.33	74.38	81.84	78.17	84.96	91.94
380mm	79.91	75.91	68.73	78.18	72.41	77.97	79.91
400mm	76.07	74.07	66.83	77.00	70.49	75.61	77.00

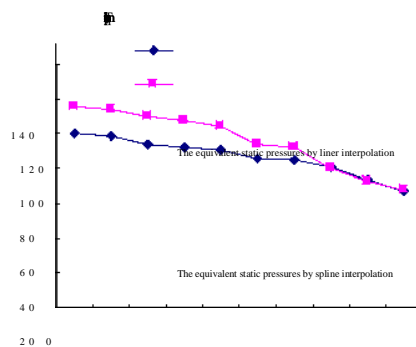


Figure 8. The maximum equivalent static pressures by Interpolation at the key parts

The equivalent static pressures by spline interpolation are generally higher than the linear interpolation in figure 8. Considering the aircraft safety, the higher results by spline interpolation as the design bases for the key parts should be selected. The interpolation method based on the shock wave propagation law is at the distance more than 500mm away from the spout. As the shock wave propagation law may be different near or far away from the spout, the data from the interpolation still need to be tested within 500mm shock wave to verify through the improvement of test conditions.

4. Conclusions

1) The maximum equivalent static pressure of the shock wave outside 500mm from the spout decreases with an increasing distance between measuring point and the spout in the tests.

2) The equivalent static pressures distributions by the linear interpolation are uniformed form of the cloud charts. The pressure distribution is smoothed by spline interpolation, but the higher pressure area is relatively concentrated.

3) The equivalent static pressures by spline interpolation are generally higher than the linear interpolation at the key parts. Considering the aircraft safety, the higher results by spline interpolation as the design bases for the key parts will be selected.

References

- [1] J. Bai, X. P. Dong and W. Wang, Rubber Industry, vol. 58, no. 11, (2011), pp. 658.
- [2] Y. M. Jiang, Y. J. Liu and P. Dai, Science & Technology Information, vol. 32, (2010), pp. 74.
- [3] L. Y. Gu and J. W. He, Aircraft Design, vol. 29, (2009), pp. 28.
- [4] C. Q. Zhao, Y. Jiang, (Eds.), "Gas Jet Dynamics", Beijing Institute of Technology, Beijing, (1998).
- [5] F. Y. Zhou, X. Q. Chen, K. Y. Zhang and F. M. Zhan, Blasting, vol. 20, no. 3, (2003), pp. 7.
- [6] D. Z. Zhang, Y. Li, F. P. Zhong, J. D. Lin, D. W. Wang and C. L. Wang, Acta Armamentarii, vol. 28, (2007), pp. 1256.
- [7] Z. Z. Sun, W. P. Yuan and Z. C. Wen, (Eds.), Numerical Analysis, Southeast University, Nanjing, (2002).
- [8] X. H. Cai, W. G., Liu and L. Y. Cai, (Eds.), MATLAB Fundamentals and Application Guide, People Post, Beijing, (2009).
- [9] S. J. Ge, Z. Z. Qiu and J. F. Lu, (Eds.), MATLAB Introduction and Practice, People Post Press, Beijing, (2008).
- [10] W. Liu, Y. Gao and S. Gao, Computer & Digital Engineering, vol. 257, (2011), pp. 21.

Authors

Runlian Jiang. An associate professor of Zhenjiang Watercraft College of PLA. Runlian Jiang is, moreover, a professional Mechanics student with PhD degree of the PLA University of Science and Technology. She is mainly engaged in the research work of mechanics and mechanical aspects. She published more than 15 articles.

Yaohua Wang. Yaohua Wang is the chief professor of the PLA University of Science and Technology. He is a doctoral tutor. Professor Yaohua Wang has long been engaged in materials synthesis and explosive processing engineering research. He has obtained 21 invention patents, two National Technology Invention Prize 2 and completed a number of major high-quality research projects as a project leader. as a project leader for high quality completed a number of major scientific research projects.

Chengfei Fan. Chengfei Fan is a professional Mechanics student with PhD degree of the PLA University of Science and Technology. He is mainly engaged in the research work of mechanics aspects. He published 8 articles.

Mianjun Duan. Mianjun Duan is a professional Mechanics student with PhD degree of the PLA University of Science and Technology. He is mainly engaged in the research work of mechanics aspects. He published 4 articles.